Gold Modified Zeolite: An Efficient Heterogeneous Catalyst for *N*-Arylation of Indazole

P. Emayavaramban[1], K. Kadirvelu[2], and N. Dharmaraj[1,*]

[1] *Inorganic and Nanomaterials Research Laboratory, Department of Chemistry, Bharathiar University, Coimbatore 641046, India*
[2] *Defence Research Development Organization—Bharathiar University, Center for Life Sciences,
Bharathiar University Campus, Coimbatore 641046, India*

We herein report *N*-arylation of indazole with aryl halides using gold modified zeolites (Au-zeolites) as an efficient catalytic system. Au-zeolites with three different gold loading were prepared by ion-exchange method and characterized by UV-visible diffuse reflectance spectroscopy (UV-DRS), transmission electron microscopy and energy-dispersive X-ray spectroscopy (TEM-EDX) and X-ray photoelectron spectroscopy (XPS). The Brunauer-Emmett-Teller (BET) and Langmuir surface areas of the prepared Au(5)-zeolite catalyst were found to be 644 and 929 m^2g^{-1} respectively. Gold-modified zeolites performed as an efficient catalytic system for *N*-arylation of indazole using diverse aryl halides afforded *N*1 arylated products in appreciable yield under mild reaction conditions. The catalyst was reusable for at least five times with only a marginal loss of activity. This simple, effective and environmentally benign heterogeneous protocol provides a safer alternative to hazardous, corrosive and more polluting conventional catalysts.

Keywords: Zeolites, Gold Modification, Aryl Indazole, *N*-Arylation, Heterogeneous Catalyst.

1. INTRODUCTION

Nitrogen heterocycles such as quinazoline, quinoline, indole, indazole etc., isolated from natural products showed prominent medicinal properties.[1] Among them, *N*-aryl-indazoles exhibited various therapeutic properties as listed in the following Table I.

From the synthetic viewpoint, direct arylation and alkenylation of the nitrogen atom present in nitrogen heterocycles are a difficult task. For example, synthesis of *N*-aryl-indazoles include cyclization of arylhydrazones of 2-bromoaldehydes and 2-bromoacetophenones and diazotization of 2-alkylaniline.[7,8] Dell'Erba et al. investigated a base promoted cyclization of (*O*-alkylaryl)azosulfides derived from 2-alkylaniline and $[3+2]$ cycloadditions of arynes with diazo compounds or hydrazones using copper or palladium catalysts.[9,10] Ullmann coupling is a well known reaction for cross-coupling of N–H heterocycles with aryl lead, aryl bismuth, aryl borane and aryl silane reagents using copper salts as a catalyst.[11–14] However, Ullmann coupling reactions has serious limitations such as elevated temperatures, extended reaction time, low tolerance functional groups and multiple

steps. Moreover, excess quantity of copper reagents is needed.

Recently, researchers have found that metal nanoparticle catalysts can be used to achieve facile synthesis of *N*-aryl-indazoles. For instance, Ganesh Babu et al. reported a simple, effective, ligand free and reusable heterogeneous catalyst for *N*-arylation of benzimidazole with copper oxide nanoparticles.[15] In addition, Yong et al. studied *N*-arylation of a series of nitrogen-containing heterocycles using Cu_2O and tetrabutylammonium bromide (TBAB) catalyst in water.[16] The Cu-catalyzed *N*-arylation of pyrazole or indazole with aryl halides using flash vacuum photolysis and microwave-based heating yielded *N*-alkylated and *N*-bromoalkenylated pyrazole or indazole.[17,18] Further, Corma and co-workers have reported Suzuki and Sonogashira cross-coupling reactions using Au(I) and Au(III) complexes as catalysts.[19] Many researchers have reported cross-coupling reactions between aryl halides and phenylboronic acids with gold nanoparticles supported on MgO as catalysts.[20,21] Hence, synthesis of *N*-aryl-indazoles by simple methodology is still a challenging task for organic chemists.

Zeolites have unique adsorption and ion-exchange properties and proved its importance in the petroleum refining

---

*Author to whom correspondence should be addressed.

Table I. Some of the biologically important *N*-aryl-indazoles.

Compound name	Structure	Biological properties	Reference
Benzydamine		analgesic, antipyretic and anti-inflammatory	2,3
N-[[1-(2-Methoxyphenyl)-1*H*-indazol-5-yl]methyl]-2-propylpentanamide		smoothened antagonists and antitumor agent	4
3-(5'-hydroxymethyl-2'-furyl)-1-benzylindazole		anti-cancer agent	5
4-aryl-1-(indazol-5-yl)pyridin-2(1*H*)ones		anti-obesity agent	6

and organic synthesis.[22] In addition, zeolites have large surface area, thermal stability and well-defined microporous structures.[23, 24] Among the zeolites, Y zeolite is used as cracking catalyst because of higher activity and stability even at high temperatures due to the higher Si/Al ratio.[22] Y zeolite is a faujasite (FAU) type, crystalline, microporous aluminosilicate with typically 0.4–1.2 nm size and built from infinitely extending three-dimensional network of SiO_4 and AlO_4 tetrahedra that are linked together through oxygen bridges.[25] The presence of Al^{3+} instead of Si^{4+} creates a negative charge, which is compensated by exchangeable transition-metal cations, after dehydration it may occupy different sites in zeolite.[26] Modification of zeolites by different metal ions is one of the methods to improve electronic and catalytic characteristics of supported metal nanoparticles.[27] Lakshmi Kantam et al. synthesised *N*-aryl hetrocycles with aryl halides by copper exchanged NaY zeolite catalyst with excellent yields under mild reaction conditions.[28]

Hence, in this paper, we describe the preparation of gold modified zeolite (Au-zeolite) by simple ion-exchange method to utilize as a heterogeneous and reusable catalyst for synthesis of *N*-arylated indazoles. To the best of our knowledge, this is the first report on the application of gold modified zeolite as a catalyst for *N*-arylation of indazoles.

2. EXPERIMENTAL DETAILS

2.1. Materials

Sodium Y zeolite (ion exchangeable zeolite) and hydrogen tetrachloroaurate $[HAuCl_4] \cdot 3H_2O$ were purchased from Aldrich chemicals. All other chemicals used were of analytical grade and used without further purification. Deionized water was prepared by water purification system. All glasswares and Teflon coated magnetic stir bars were washed with aqua regia, followed by copious rinsing with deionised water before drying in an oven at 150 °C.

2.2. Preparation of Gold Modified Zeolite (Au-Zeolite)

In a 250 mL round bottom flask, 1 g of sodium Y zeolite and 100 mL of an aqueous solution containing different molar concentration of $[HAuCl_4] \cdot 3H_2O$ were taken (1 mM, 3 mM and 5 mM) and the resulting slurry was stirred for 24 h in nitrogen atmosphere at room temperature. The Au^{3+}-exchanged Y zeolite (Au^{3+}-zeolite) was filtered using Whatman-1 filter paper and the residue (Au^{3+}-Y zeolite) was rinsed with deionised water to remove chloride ions. The resulting Au^{3+}-Y zeolite was dried under vacuum overnight. The prepared samples were calcined in muffle furnace at 400 °C for 5 h. The obtained gold modified Y zeolite catalysts were named as Au(1)-zeolite, Au(3)-zeolite and Au(5)-zeolite respectively, according to different gold content.

2.3. Characterization

UV-visible spectra of the Au-zeolites were recorded with a double beam UV/vis. and UV-DRS-JASCO (model V550) spectrophotometer. Powder X-ray diffraction (XRD) patterns were recorded with a PAN analytical X'PERT-PRO diffractometer using Cu Kα radiation (wavelength 1.54056 Å, 40 kV, 55 mA). Fourier transform infrared spectra (FT-IR) were recorded using KBr pellets on a JASCO FT-IR-460 spectrophotometer in the range of 4000–400 cm^{-1}. Raman spectra of the samples were recorded from a laser Raman spectrometer (Horiba Jobin-LabRam-HR-UV) using a 20 mW argon laser operating at 514 nm. Field emission scanning electron microscopic (FE-SEM) images were taken using a FEI Quanta 250 at 30 kV and 33 Pa in a low-vacuum mode without metal coating on aluminium support. Transmission electron microscopy (TEM) was performed on a JEM-2100 F microscope (JEOL) operating at 200 kV. Elemental analysis was performed by an energy dispersive X-ray (EDX) analyzer attached with TEM instrument. XPS analysis was performed on a Physical Electronics 5800 spectrometer equipped with a hemispherical analyzer and using monochromatic Al Kα radiation (1486.6 eV, the X-ray tube working at 15 kV and 350 W) and pass energy of 23.5 eV. The nitrogen adsorption/desorption experiments were carried out at 77 K using an ASAP 2020 system of micromeritics the autosorp-iQ (Quantachrome instruments). Gold content of the modified zeolite catalysts were determined by inductively coupled plasma atomic emission spectroscopy (ICP-AES) using a PerkinElmer, optima 3000 model. ICP-AES samples prepared by dissolving Au-zeolites in a mixture of HCl/HNO$_3$ (3:1), to make clear solution adequate amount of HF solution added and then solutions were kept in microwave digester for 20 min. Thermogravimetric and differential thermal analyses (TG-DTA) were recorded in a PerkinElmer Pyris Diamond TG/DTA under nitrogen atmosphere with a heating rate of 10 °C per min. The sample was de-gassed under vacuum at 423 K for 24 h before the adsorption of nitrogen. The product conversion was quantified by PerkinElmer Clarus
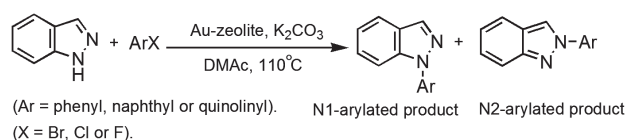
Scheme 1. Au-zeolite catalyzed *N*-arylation of indazole with aryl halides.

600 gas chromatography and mass spectroscopy (GC-MS). Nuclear magnetic resonance (NMR) spectra were recorded in $CDCl_3$ with BRUKER AMX 500 at 500 MHz with tetra methyl silane as an internal standard.

2.4. GC-MS Analysis

GC-MS analysis was carried out by PerkinElmer Clarus 600 gas chromatograph/mass spectrometer instrument equipped with a 5% diphenyl and 95% dimethyl polysiloxane, Restek-5 capillary column (60 m length, 0.32 mm dia). GC was coupled with MSD and triple axis mass selective ion detector. The initial temperature was kept at 50 °C and reached a maximum of 280 °C. One μL of sample was injected with split mode (10:1). Helium used as a carrier gas at flow rate of 0.8 mL/min and the total run time was 23 mins. Electron impact mass spectrometry was performed, with electron energy of 70 eV and ion source and interface temperature of 250 °C. The acquisition was performed in scanning mode (mass range m/z 50–500). MS library (NIST-MS library) was conducted for identification of products using the database of National Institute Standard and Technology.

2.5. Procedure for *N*-Arylation of Indazole

In a typical *N*-arylation reaction, Au(5)-zeolite catalyst (100 mg) was added to a mixture of indazole (118 mg, 1 mM), 4-chlorobenzonitrile (206 mg, 1.5 mM) and K_2CO_3 (276 mg, 2.0 mM) in *N,N*-dimethylacetamide (DMAc, 4 mL) and stirred at 110 °C (Scheme 1). Completion of the reaction was monitored by thin-layer chromatography (TLC) and then the reaction mixture was centrifuged to separate the catalyst followed by several time washings with ethyl acetate. Then, the organic layer was quenched with ice and the product was extracted twice with ethyl acetate. The combined organic extracts were dried over anhydrous sodium sulphate, filtered and concentrated to a very small volume. The residue obtained was used for GC-MS analysis and purified by column chromatography on silica gel (petroleum ether/ethyl acetate, 70/30) to afford pure *N*1 and *N*2 arylated products.

3. RESULTS AND DISCUSSION

Three different samples of gold modified Y zeolites were prepared by two step processes as described below.
(i) Au^{3+} ions was exchanged with sodium Y zeolite by ion exchange method and

(ii) reduction of Au^{3+} ions to gold modified Y zeolite support was achieved by the thermal process.

The optical properties of Au-zeolite(1), Au-zeolite(3) and Au-zeolite(5) were studied and are shown in Figure 1, where the ability of Au^{3+} ions to exchange with sodium Y zeolite was found to increase with increasing concentration of gold solution from 1 mM, 3 mM and 5 mM. The characteristic surface plasmon resonance band (SPR) for gold nanoparticles was observed at 526 nm.[29] In absence of gold no characteristic SPR band was identified for (a) sodium Y zeolite. The band (b) showed a weak absorption due to the presence of low content of gold and it is well supported by ICP-AES analysis (Table II). On the other hand, the sharp SPR bands were observed in (c) and (d) curves. However, an increase in the intensity of absorption bands was observed without any shift in the position of SPR bands upon increasing the concentration of gold solution.

Figure 2 displays a comparison of XRD patterns of sodium Y zeolite, Au^{3+}-exchanged Y zeolite and gold modified Y zeolite (Au(5)-zeolite). However, the XRD patterns did not show any noticeable change in both the intensities and positions of the Bragg peaks, indicating that neither the crystallinity nor the lattice of Y zeolite was altered by ion exchange with Au^{3+} ions followed by thermal process.[30] The XRD patterns did not show any diffraction due to AuNPs because of its very low content in Au-zeolites.

FT-IR spectra of the Au-zeolites were recorded to identify structural stability of the material after modification from sodium form of Y zeolite to gold form of Y zeolite and are shown in Figure 3. The spectra of Y zeolite before and after gold loading were recorded to understand the stability of the samples. The strong bands observed at 3469 and 1642 cm^{-1} were assigned to hydroxyl groups present in framework of the Y zeolite and other bands at 581 and 473 cm^{-1} were related to six membered rings which is a key structural feature of FAU type (sodium
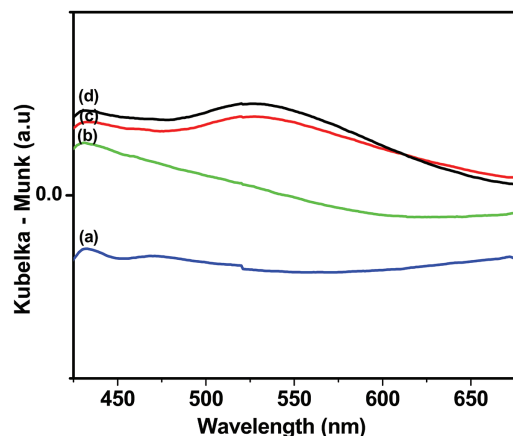

Figure 1. UV-DRS spectra of (a) sodium Y zeolite, (b) Au(1)-zeolite, (c) Au(3)-zeolite and (d) Au(5)-zeolite.

Table II. Amount of gold loaded on sodium Y zeolite.[a]

S. no.	Concentration of Au^{3+} solution (mM)	Au loading on sodium Y zeolite (ppm)
1	1	0.0237
2	3	0.5863
3	5	0.7520

Note: [a] Au content measured by ICP-AES.

Y zeolite) framework.[31, 32] However, there was no predominate changes in FT-IR spectra during the modification as well as gold ion exchange processes.

Raman spectroscopy was recorded to characterize sodium Y zeolite and Au(5)-zeolite. The spectrum of sodium Y zeolite and Au(5)-zeolite are given in Figure 4. From Raman spectra of the samples, interaction between gold and zeolite was identified. The sodium Y zeolite displayed sharp bands at 505 cm^{-1} and 300 cm^{-1} which were assigned to the T–O–T (T = Si/Al) bending vibration of zeolite framework.[33–35] In contrast, the Au(5)-zeolite showed only weak absorption band at these wavelengths probably due to the fluorescence quenching from gold on the surface of zeolite.[36]

The morphology and composition of gold modified Y zeolite were investigated by FE-SEM, TEM-EDX and ICP-AES analysis. FE-SEM images of gold modified Y zeolite shown in Figures 5(a–d) revealed that
(i) there exist only crystals of Y zeolite,
(ii) there was no bulk metal outside the zeolite crystals and
(iii) the method used for the preparation of gold modified does not cause any observable defects in the structure of Y zeolite.

These results were also supported by XRD results. The TEM image of gold modified Y zeolite and its TEM-EDX

Figure 3. FT-IR spectra of (a) sodium Y zeolite, (b) Au^{3+} ion-exchanged Y zeolite and (c) Au(5)-zeolite.

spectrum are given in Figures 6(a and b). The presences of gold nanoparticles are not seen in TEM images. But, it was as identified through TEM-EDX and further it was supported by ICP-AES results. In addition, the zeolite framework elements Si, Al, O, Na and Cu from the grid were also observed in the EDX.

X-ray photoelectron spectroscopy (XPS) provides further insight into the oxidation state of gold in Au(5)-zeolite and the elemental composition. Figure 7 shows the XPS spectrum of Au(5)-zeolite and the peaks for possible elements such as Al 2*p*, Si 2*p* and O 1*s* were observed at binding energies of 74, 102.8 and 532 eV respectively.[37] In addition, very small peaks were found at 84 and 88 eV due to the presence of gold nanoparticles.[38] However, the above peaks for metallic gold are not clear due to less content of gold on the surface of zeolite.

N_2-adsorption/desorption isotherms of Au(5)-zeolite presented in Figure 8 showed type I nature, a characteristic of microporous materials. The micropore volume and

Figure 2. XRD patterns of (a) sodium Y zeolite, (b) Au^{3+} ion-exchanged Y zeolite and (c) gold modified Y zeolite (Au(5)zeolite) after thermal treatment.
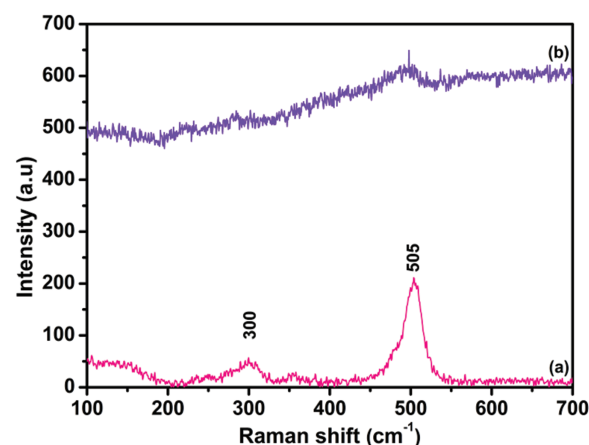
Figure 4. Raman spectra of (a) sodium Y zeolite and (b) Au(5)-zeolite.
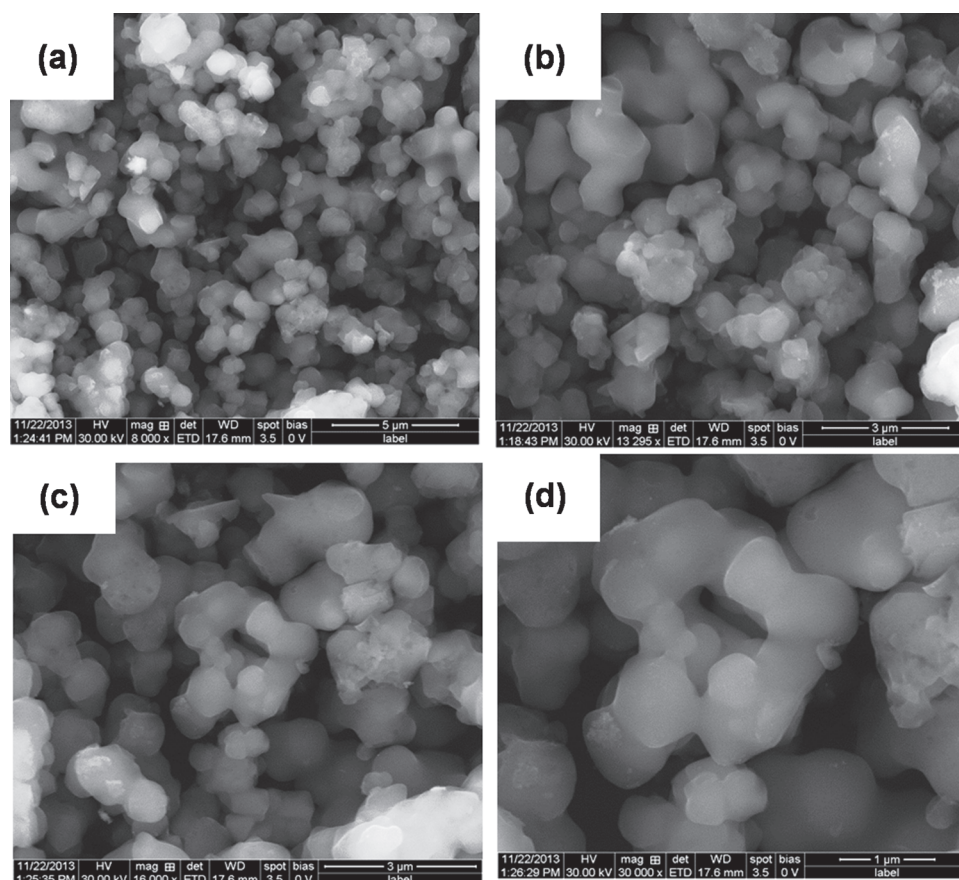
Figure 5. FE-SEM images of Au(5)-zeolite (a–d) (from lower magnification to higher magnification).

surface area of Au(5)-zeolite determined by DFT method were found to be 0.323 cm^3g^{-1} and 1108.2 m^2g^{-1}. The BET and Langmuir surface area of the prepared Au(5)-zeolite catalyst were found to be 644.5 and 929.4 m^2g^{-1} respectively (Fig. 9). Then, the pore size derived from the N_2-adsorption isotherms using DFT method suggested the average pore size of the Au(5)-zeolite was ∼0.614 nm (Fig. 10).

A thermogravimetric (TG) (Fig. 11) analysis was carried out to study the weight loss and stability of Au(5)-zeolite. Initially, the TG curve showed 22% of weight loss up

to 200 °C, attributed to the surface water molecules in zeolite matrix. But, above 200 °C there was no predominant weight loss occurred even up to 800 °C indicating the stability of Au(5)-zeolite. The obtained DTA curve showed an exothermic peak at 200 °C due to the removal of surface bound water molecules present in Au(5)-zeolite.

3.1. Catalytic Test
3.1.1. Optimization of Reaction Conditions
To identify suitable conditions for catalytic studies, the parameters such as substrate-catalyst ratio, solvent, nature
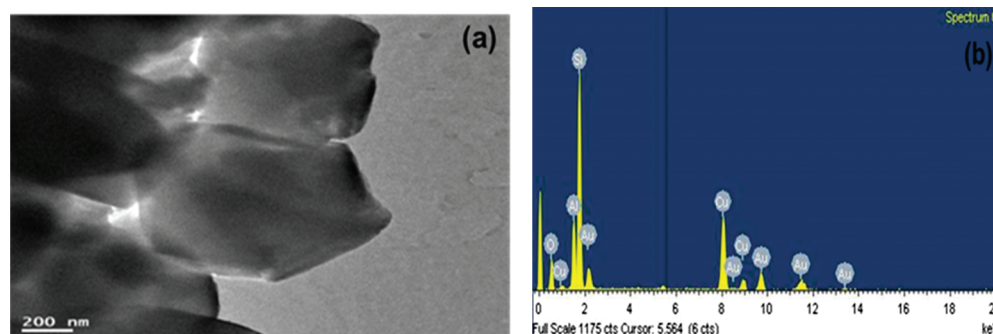
Figure 6. (a) TEM image of an individual matrix of Au(5)-zeolite and (b) corresponding EDX spectrum.
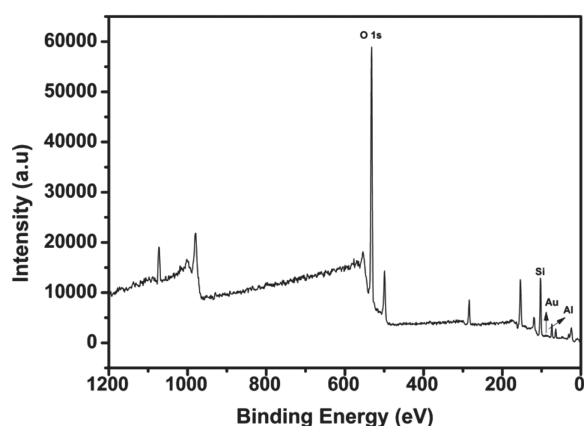
Figure 7. XPS spectrum of Au(5)-zeolite.
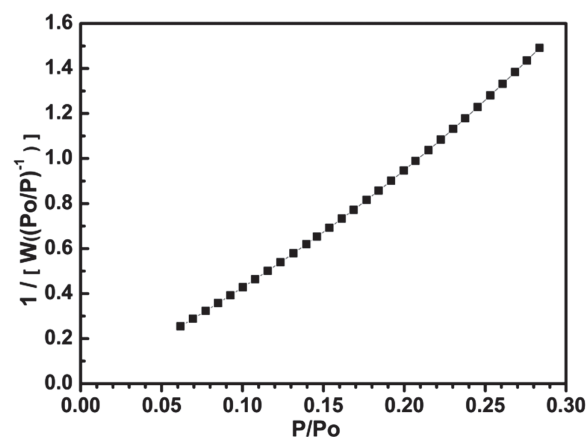
Figure 9. Multipoint BET surface area of Au(5)-zeolite.

and quantity of base and mole percent of gold in the catalyst were optimized. Hence, the reaction between indazole and 4-chlorobenzonitrile was carried out at different reaction conditions. From the data given in Table III, it was concluded that among the five solvents (acetonitrile, toluene, tetrahydrofuran (THF), water and *N*,*N*-dimethylacetamide (DMAc)), only DMAc produced higher yield of the product (100%) and hence, it was chosen for all the reactions (Table III, entries 8–12). Similarly, four different bases such as potassium carbonate (K_2CO_3), potassium hydroxide (KOH), potassium phosphate (K_3PO_4) and potassium *tert*-butoxide ((CH_3)$_3$COK) were tested for their performance in the above catalysis reactions. Among them, potassium carbonate (2 mM) was found to be an effective base (Table III, entries 8, 13–16). Moreover, Au(5)-zeolite showed better catalytic activity than the other two catalysts (Au(3)-zeolite and Au(1)-zeolite) (Table III, entries 2, 3 and 8). However, the same reaction conducted with sodium Y zeolite as catalyst yielded only 10% of product (Table III, entry 1), which indicated that the presence of Au in the chosen catalytic system is mainly responsible for its activity in *N*-arylation. Further, upon increasing the quantity of base added in this

reaction from 0.5 to 2.0 mM produced higher yields of the *N*-arylated compounds. But, addition of 2.5 mM quantity of the base caused a negative effect and decreased the product yield (Table III, entries 5–8). Finally, *N*-arylation of indazoles was successfully carried out under the optimized reaction conditions involving aryl halide (1.5 mM), indazole (1 mM), K_2CO_3 (2 mM) and 100 mg of Au(5)-zeolite as catalyst in DMAc as solvent at 110 °C.

3.1.2. Extension of Scope

Scope of the present catalytic system (Au(5)-zeolite) to a series of reaction between indazole and various aryl halides was tested. In majority of the cases, arylated products were obtained in appreciable yields (Table IV) and compared with earlier reported catalytic systems for the same reaction to obtain *N*-arylated indazole.[16, 39] Among the halogens, the bromo group was one of the best leaving groups as compared to the chlorine and fluorine (leaving group ability of halogens was in the order of Br > Cl > F) and hence, the aryl bromides reacted faster than the respective aryl chlorides and fluorides.[40] Usually C–F bond activation is not so easy because of poor
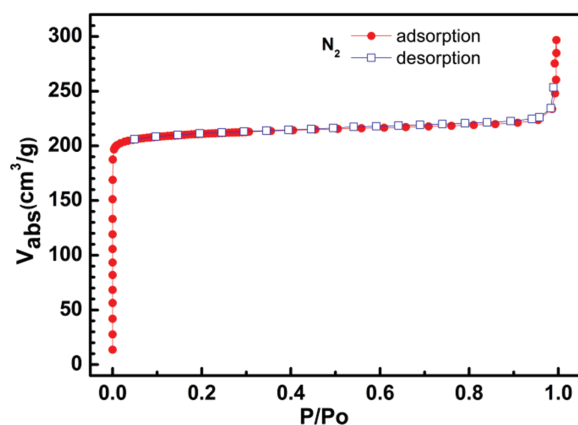
Figure 8. N$_2$-adsorption/desorption isotherms of Au(5)-zeolite.
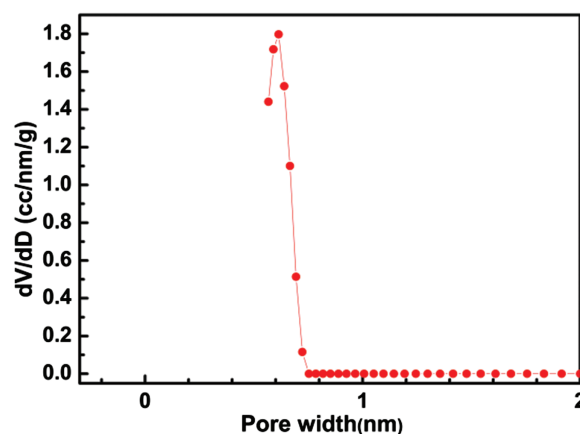
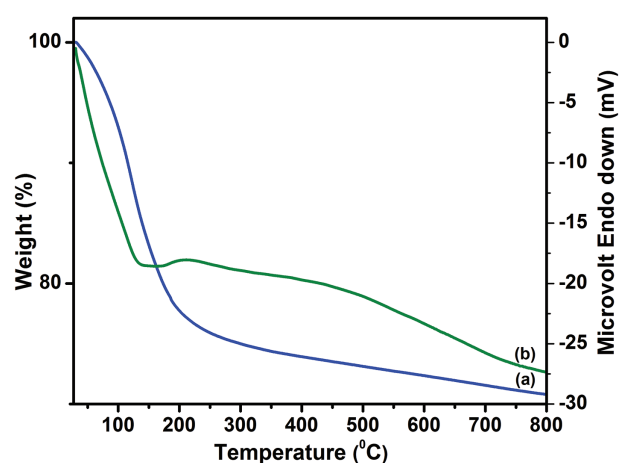**Figure 10.** Pore size distributions of Au(5)-zeolite evaluated by the DFT method.

Figure 11. (a) TG and (b) DTA curves of Au(5)-zeolite.

leaving group ability of the fluoride. As the electron withdrawing effect of the substituent at the phenyl ring of aryl halides increases, the reactivity towards *N*-arylation also increases (Table IV, entries 1–3). On the other hand, *ortho*-substituted aryl halides gave poor yield for Br > Cl > F compared to the *para*-substituted aryl halides due to the steric effect of cyano group at the *ortho* position (Table IV, entries 4–6). Since nitro group is one of the strongest electron withdrawing group, the aryl halide possessing such substituent gave better yield compared to trifluoromethyl substituted compounds ($-CF_3$) (Table IV, entries 7–9). When *N*-arylation of indazole and aryl halides with electron donating groups were carried out, lower yield of arylated products were obtained compared to electron withdrawing substituent. The ratio of $N1:N2$ products was higher for 4,7-dichloroquinoline

Table III. Optimization of reaction conditions for *N*-arylation of indazole.[a]

Entry	Catalyst	Solvent	Base (mM)	Total yield $N1 + N2$ (%)[b]
1	Y zeolite	DMAc	K_2CO_3 (2.0)	10
2	Au(1)-zeolite	DMAc	K_2CO_3 (2.0)	20
3	Au(3)-zeolite	DMAc	K_2CO_3 (2.0)	90
4	Au(5)-zeolite	DMAc	K_2CO_3 (2.5)	96
5	Au(5)-zeolite	DMAc	K_2CO_3 (0.5)	72
6	Au(5)-zeolite	DMAc	K_2CO_3 (1.0)	88
7	Au(5)-zeolite	DMAc	K_2CO_3 (1.5)	96
8	Au(5)-zeolite	DMAc	K_2CO_3 (2.0)	100
9	Au(5)-zeolite	Acetonitrile	K_2CO_3 (2.0)	80
10	Au(5)-zeolite	Toluene	K_2CO_3 (2.0)	76
11	Au(5)-zeolite	Water	K_2CO_3 (2.0)	–
12	Au(5)-zeolite	THF	K_2CO_3 (2.0)	57
13	Au(5)-zeolite	DMAc	Na_2CO_3 (2.0)	92
14	Au(5)-zeolite	DMAc	K_3PO_4 (2.0)	32
15	Au(5)-zeolite	DMAc	KOH (2.0)	56
16	Au(5)-zeolite	DMAc	$(CH_3)_3COK$ (2.0)	87

Note: [a]Reaction condition: Indazole (1 mM, 118 mg), ArX (1.5 mM), K_2CO_3, 100 mg of Au(5)-zeolite in 4 mL of DMAc at 110 °C for 24 h; [b]GC-MS yield.

than 2,4,7-trichloroquinoline (Table IV, entries 10 and 11). 1-Bromonaphthalene gave lower yield due to an absence of activating groups (donating or withdrawing groups) in the ring (Table IV, entry 12).[40] Interestingly, higher yield of *N*-aryl indazole was obtained when 4-bromobenzophenone and 4-chlorobenzophenone were used as aryl halides as presented in Table IV, entries 13 and 14.

Sheldon test was performed to identify any possible leaching of gold nanoparticles from Au(5)-zeolite during catalysis.[41] The obtained results clearly indicated that there was no appreciable leaching of gold nanoparticles under the present reaction conditions. The absence of leaching is further confirmed from ICP-AES analysis of the filtrate from the reaction mixture and also of the filtrate from a stirred solution of Au(5)-zeolite in DMAc for 24 h at 110 °C.

Simultaneously, the recovery and reusability of Au(5)-zeolite were also investigated (Table V). After completion of the reaction, products were extracted with ethyl acetate, dried over anhydrous sodium sulphate and concentrated. Au(5)-zeolite was washed three times with ethyl acetate, filtered and air dried prior to reuse. After each cycle, the recovered Au(5)-zeolite retained its activity and afforded 92% yield after the fifth cycle. ICP-AES analysis of the reused Au(5)-zeolite confirmed the presence of 0.752 ppm of gold and supported the heterogeneous nature of Au(5)-zeolite.

3.2. Mechanism

The mechanism proposed for Au(5)-zeolite catalyzed *N*-arylation of indazole with aryl halide is given in Figure 12. In the first step, aryl halide was adsorbed on the surface of the gold modified Y zeolite. The excess charge generated due to this adsorption could be shared among the gold atoms. Then it undergoes a reaction with indazole that has two tautomeric forms $N1$ and $N2$ in basic medium and the catalytic cycle was completed by the elimination of *N*-arylated indazoles.

3.3. FT-IR, GC-MS, ¹H and ¹³C NMR Spectral Data

(In the interpretation of NMR data, following abbreviations are used: s-singlet, t-triplet, m-multiplet and *J*-coupling constant).

3.3.1. 1-(Benzophenone-4-yl)-1H-Indazole (Table IV, Entry 14, N1-Arylated Product)

¹H NMR (500 MHz, $CDCl_3$): δ 7.29 (t, 1H, $J = 7.5$ Hz, Ar-H), 7.48–8.02 (m, 10H, Ar-H), 8.26 (s, 1H, CH=N) ppm.

¹³C NMR (125 MHz, $CDCl_3$): δ 110.7 (–CH), 121.5 (–CH), 121.7 (–CH), 122.3 (–CH), 126.0 (–C), 127.9 (–CH), 128.5 (–CH), 130.1 (–CH), 131.8 (–CH), 132.6 (–CH), 135.1 (C), 136.8 (–C), 137.7 (–C), 138.8 (–C), 143.7 (–CH), 195.7 (C=O) ppm.

FTIR (KBr): v_{max} 1643 cm^{-1}; GC-MS m/z: 291 (M$^+$).

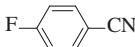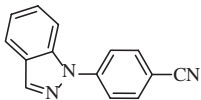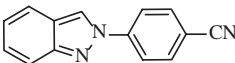**Table IV.** Au(5)-zeolite-catalyzed *N*-arylation of indazole with various aryl halides.[a]
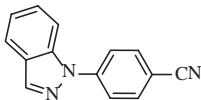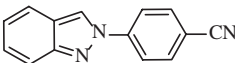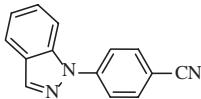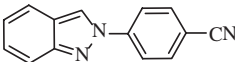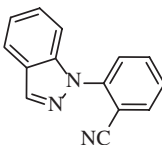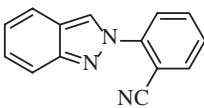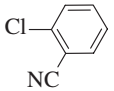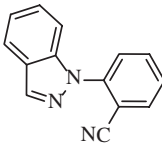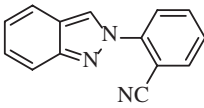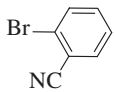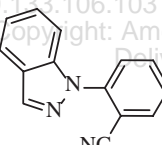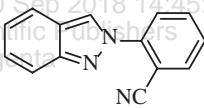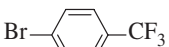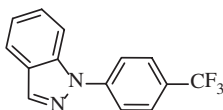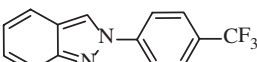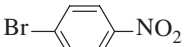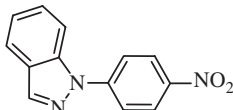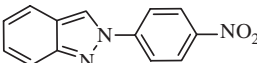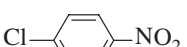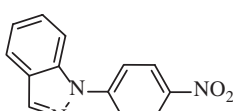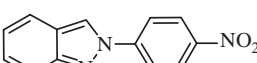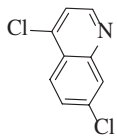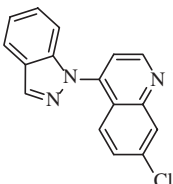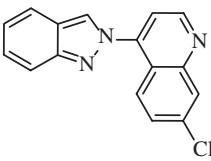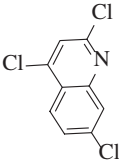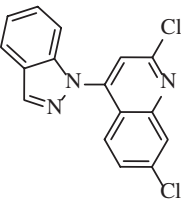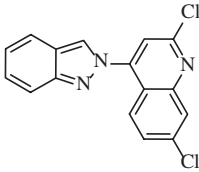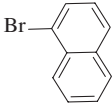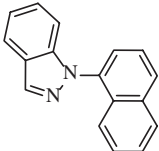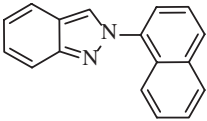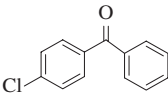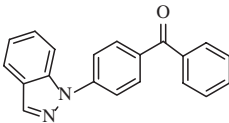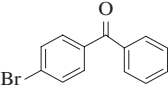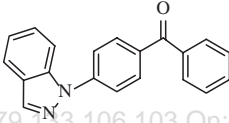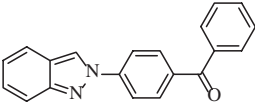
Entry	Aryl halide	N1 Arylated Product	N2 Arylated Product	Yield (%)[b]	Product	
					N1	N2
1	F—⬡—CN			100	58	42
2	Cl—⬡—CN			100	64	36
3	Br—⬡—CN			100	60	40
4	F / NC			100	68	32
5	Cl / NC			70	40	30
6	Br / NC			49[c]	26	23
7	Br—⬡—CF₃			7	4	3
8	Br—⬡—NO₂			82	62	20
9	Cl—⬡—NO₂			100[c]	60	40
10	Cl / Cl quinoline			100	51	49

Table IV. Continued.

Entry	Aryl halide	N1 Arylated product	N2 Arylated product	Yield (%)[b]	Product N1	Product N2
11				92	56	36
12				12	10	2
13				98	54	44
14				100[c]	52	48

Notes: [a]Reaction condition: Indazole (1 mM, 118 mg), ArX (1.5 mM), K$_2$CO$_3$ (2 mM, 276 mg), Au(5)-zeolite (100 mg) in 4 mL of DMAc at 110 °C for 24 h; [b]GC-MS yield; [c]Isolated yield after column chromatography.

3.3.2. 2-(Benzophenone-4-yl)-2H-Indazole (Table IV, Entry 14, N2-Arylated Product)

^{1}H NMR (500 MHz, CDCl$_3$): δ 7.12–8.08 (m, 13H, Ar-H), 8.52 (s, 1H, CH=N) ppm.
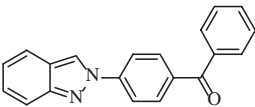
^{13}C NMR (125 MHz, CDCl$_3$): δ 118.1 (–CH), 120.4 (–CH), 120.6 (–CH), 120.7 (–C), 123.1 (–CH), 123.2 (–CH), 127.7 (–CH), 128.6 (–CH), 130.1 (–CH), 131.8 (–C), 132.8 (–CH), 136.8 (–C), 137.5 (–C), 143.3 (–C), 150.3 (–C), 195.6 (–C=O) ppm.

FTIR (KBr): v_{max} 1643 cm^{-1}; GC-MS *m/z*: 291 (M$^+$).

3.3.3. 1-(4-Nitrophenyl)-1H-Indazole (Table IV, Entry 9, N1-Arylated Product)

^{1}H NMR (500 MHz, CDCl$_3$): δ 7.32 (t, 1H, *J* = 7.0 Hz, Ar-H), 7.51–7.98 (m, 5H, Ar-H), 8.27 (s, 1H, CH=N) 8.38 (d, 2H, *J* = 4.0 Hz, Ar-H) ppm.

Table V. Reusability of Au(5)-zeolite for *N*-arylation of indazole with 4,7-dichloroquinoline.[a]

Cycle	First	Second	Third	Forth	Fifth
Yield (%)[b]	98	97	97	96	92

Note: [a]Reaction condition: Indazole (1 mM, 118 mg), ArX (1.5 mM), K$_2$CO$_3$ (2 mM, 276 mg), Au(5)-zeolite catalyst (100 mg) in 4 mL of DMAc at 110 °C for 24 h; [b]GC-MS yield.

^{13}C NMR (75 MHz, CDCl$_3$): δ 110.6 (–CH), 119.4 (–C), 121.5 (–CH), 122.0 (–CH), 122.8 (–CH), 125.5 (–CH), 128.4 (–CH), 137.7 (–CH), 138.7 (–C), 145.2 (–C), 145.5 (–C) ppm.
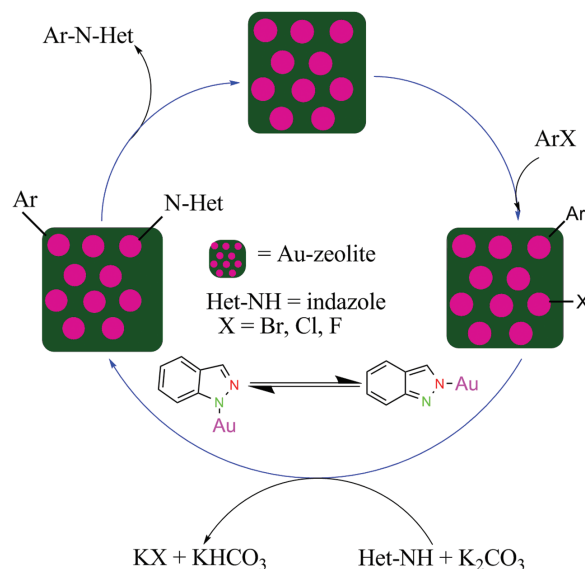
Figure 12. Proposed mechanisms for Au(5)-zeolite catalyzed *N*-arylation of indazole with aryl halides.

FTIR (KBr): v_{max} 1511 cm^{-1} (asym, $-NO_2$), v_{max} 1336 cm^{-1} (sym, $-NO_2$); GC-MS m/z: 239 (M$^+$).

3.3.4. 1-(2-Cyanophenyl)-1H-Indazole (Table IV, Entry 6, N1-Arylated Product)

^{1}H NMR (500 MHz, CDCl$_3$): δ 7.30 (t, 1H, $J =$ 8 Hz, Ar-H), 7.49–7.94 (m, 7H, Ar-H), 8.25 (s, 1H, CH=N) ppm.

^{13}C NMR (75 MHz, CDCl$_3$): δ 109.5 (–C), 110.5 (–CH), 118.0 (–CH), 118.6 (–C), 121.9 (–C), 122.0 (–CH), 122.6 (–CH), 126.3 (–C), 128.2 (–CH), 133.7 (–CH), 137.4 (–CH), 138.7 (–C) ppm.

FTIR (KBr): v_{max} 2222 cm^{-1} (-CN); GC-MS m/z: 219 (M$^+$).

4. CONCLUSION

In summary, Au-zeolites with different content of gold were prepared by an ion-exchange method and characterized by various analytical techniques. UV-DRS spectrum of the prepared Au-zeolites exhibited the surface plasmon resonance at 526 nm, which is characteristic feature of gold nanoparticles. TEM image clearly indicated the well crystalline nature of gold modified zeolite and absence of any defects in the crystals. Though we could not detect gold nanoparticles on the surface of zeolite crystals, EDX measurement confirmed the presence of gold in them. Nitrogen adsorption/desorption and BET surface area analysis revealed that the microporous nature of the catalyst with an average surface area of 644 m^{2}g^{-1}. From the application point of view of the newly prepared catalyst, Au-zeolite was used as an efficient heterogeneous catalyst for *N*-arylation of indazoles with various substituted aryl halides in presence of K$_2$CO$_3$ and DMAc at 110 °C. Reusability of gold modified zeolite was tested for five cycles and it's stability against leaching of gold was confirmed by ICP-AES. The *N*-arylated heterocyclic products obtained in this study were characterized by ^{1}H, ^{13}C NMR spectroscopy and GC-MS analysis.

References and Notes

1. Z. Ali, D. Ferreira, P. Carvalho, M. A. Avery, and I. A. J. Khan, *Nat. Prod.* 71, 1111 (**2008**).
2. L. Mosti, G. Menozzi, P. Schenone, D. Cervo, G. Esposito, and E. Marmo, *Farmaco* 45, 415 (**1990**).
3. A. Thangadurai, M. Minu, S. Wakode, S. Agrawal, and B. Narasimhan, *Med. Chem. Res.* 21, 1509 (**2012**).
4. G. Dessole, D. Branca, F. Ferrigno, O. Kinzel, E. Muraglia, M. C. Palumbi, M. Rowley, S. Serafini, C. Steinkühler, and P. Jones, *Bioorg. Med. Chem. Lett.* 19, 4191 (**2009**).
5. Q. Zhao, J. Du, H. Gu, X. Teng, Q. Zhang, H. Qin, and N. Liu, *Pancreas* 34, 242 (**2007**).
6. M. Hadden, D. M. Deering, A. J. Henderson, M. D. Surman, M. Luche, Y. Khmelnitsky, S. Vickers, J. Viggers, S. Cheetham, and P. R. Guzzo, *Bioorg. Med. Chem. Lett.* 20, 7020 (**2010**).
7. A. Y. Lebedev, A. S. Khartulyari, and A. Z. Voskoboynikov, *J. Org. Chem.* 70, 596 (**2005**).
8. V. Collot, J. C. Ros, C. Alayrac, B. Witulski, and S. Rault, *Tetrahedron Lett.* 43, 2695 (**2002**).
9. C. Dell'Erba, M. Novi, G. Petrillo, and C. Tavani, *Tetrahedron* 50, 3529 (**1994**).
10. P. Li, J. Zhao, C. Wu, R. C. Larock, and F. Shi, *Org. Lett.* 13, 3340 (**2011**).
11. P. López-Alvarado, C. Avendaño, and J. C. Menéndez, *Tetrahedron Lett.* 33, 6875 (**1992**).
12. P. López-Alvarado, C. Avendaño, and J. C. Menéndez, *J. Org. Chem.* 61, 5865 (**1996**).
13. G. I. Elliott and J. P. Konopelski, *Org. Lett.* 2, 3055 (**2000**).
14. P. Y. S. Lam, S. Deudon, K. M. Averill, R. Li, M. Y. He, P. DeShong, and C. G. Clark, *J. Am. Chem. Soc.* 122, 7600 (**2000**).
15. S. Ganesh Babu and R. Karvembu, *Ind. Eng. Chem. Res.* 50, 9594 (**2011**).
16. F.-F. Yong, Y.-C. Teo, S.-H. Tay, B. Y.-H. Tan, and K.-H. Lim, *Tetrahedron Lett.* 52, 1161 (**2011**).
17. R. F. C. Brown, F. W. Eastwood, G. B. Fallon, S. C. Lee, and R. P. McGeary, *Aust. J. Chem.* 47, 991 (**1994**).
18. G. A. Burley, D. L. Davies, G. A. Griffith, M. Lee, and K. Singh, *J. Org. Chem.* 75, 980 (**2010**).
19. C. G. Arellano, A. Corma, and M. Iglesias, *J. Catal.* 238, 497 (**2006**).
20. V. K. Kanuru, G. Kyriakou, S. K. Beaumont, A. C. Papageorgiou, D. J. Watson, and R. M. Lambert, *J. Am. Chem. Soc.* 132, 8081 (**2010**).
21. D. K. Dumbre, P. N. Yadav, S. K. Bhargava, and V. R. Choudhary, *J. Catal.* 301, 134 (**2013**).
22. J. D. Sherman, *Proc. Natl. Acad. Sci. USA* 96, 3471 (**1999**).
23. H. S. Nalwa (ed.), Encyclopedia of Nanoscience and Nanotechnology, American Scientific Publishers, Los Angeles, CA (**2004/2011**), Vol. 1–25.
24. A. A. Elzatahry, T. A. Salah El-Din, E. A. Elsayed, D. M. Aldhayan, M. A. M. Wadaan, A. M. Al.-Enizi, and S. S. Al.-Deyab, *Sci. Adv. Mater.* 6, 1531 (**2014**).
25. K. Honda, M. Itakura, Y. Matsuura, A. Onda, Y. Ide, M. Sadakane, and T. Sano, *J. Nanosci. Nanotechnol.* 13, 3020 (**2013**).
26. V. Rama, K. Kanagaraj, and K. Pitchumani, *J. Org. Chem.* 76, 9090 (**2011**).
27. E. Smolentseva, N. Bogdanchikova, A. Simakov, A. Pestryakov, M. Avalos, M. H. Farias, A. Tompos, and V. Gurin, *J. Nanosci. Nanotechnol.* 7, 1882 (**2007**).
28. M. Lakshmi Kantam, B. Purna Chandra Rao, B. M. Choudary, and R. Sudarshan Reddy, *Synlett* 14, 2195 (**2006**).
29. P. Emayavaramban, K. Selvam, and N. Dharmaraj, *Adv. Sci. Eng. Med.* 6, 649 (**2014**).
30. J. A. Rabo, Zeolite Chemistry and Catalysis, ACS, Washington, (**1976**).
31. S. Markovic, V. Dondur, and R. Dimitrijevic, *J. Mol. Struct.* 654, 223 (**2003**).
32. N. Ninan, M. Muthiah, I-K. Park, A. Elain, T. W. Wong, S. Thomas, and Y. Grohens, *J. Biomed. Nanotechnol.* 11, 1550 (**2015**).
33. F. Fan, Z. Feng, and C. Li, *Chem. Soc. Rev.* 39, 4794 (**2010**).
34. P. K. Dutta, D. C. Shieh, and M. Prui, *J. Phys. Chem.* 91, 2332 (**1987**).
35. X. Zhang, X. Ke, and H. Zhu, *Chem. Eur. J.* 18, 8048 (**2012**).

36. E. O. Ganbold, J. H. Park, U. Dembereldorj, K. S. Ock, and S. W. Joo, *J. Raman Spectrosc.* 42, 1614 **(2011)**.
37. S. J. Kulkarni, S. Badrinarayan, and S. B. Kulkarni, *J. Catal.* 75, 423 **(1982)**.
38. A. Afzal, C. D. Franco, E. Mesto, N. Ditaranto, N. Cioffi, F. Scordari, G. Scamarcio, and L. Torsi, *Mater. Express* 5, 171 **(2015)**.

39. J. C. Antilla, J. M. Baskin, T. E. Barder, and S. L. Buchwald, *J. Org. Chem.* 69, 5578 **(2004)**.
40. P. Emayavaramban, S. Ganesh Babu, R. Karvembu, and N. Dharmaraj, *J. Nanosci. Nanotechnol.* 15, 9358 **(2015)**.
41. H. E. B. Lempers and R. A. Sheldon, *J. Catal.* 175, 62 **(1998)**.